FLAT PLATE TURBULENT BOUNDARY LAYER STATIC TEMPERATURE DISTRIBUTION WITH HEAT TRANSFER

by

Shimer Z. Pinckney III

Thesis Submitted to the Graduate Faculty of the

Virginia Polytechnic Institute

in Candidacy for the Degree of

MASTER OF SCIENCE

in

AEROSPACE ENGINEERING

APPROVED:

F. R. DeJarnette

J. B. Eades, Jr.

T. H. Chang

May 1966

Blacksburg, Virginia

TABLE OF CONTENTS

LIST OF TABLES

LIST OF FIGURES

LIST OF SYMBOLS

a — an expression given by the ratio $\dfrac{\frac{k}{C_p} + \rho \epsilon_h}{\mu + \rho \epsilon}$

b, c — constants assumed in the relationship between $\frac{q}{\tau}$ and $\left(\frac{u}{u_\infty}\right)$ (b and c are really functions of x)

C_f — friction coefficient, $\dfrac{2\tau_w}{\rho_\infty u_\infty^2}$

C_p — specific heat of a fluid at constant pressure

h — static enthalpy (for perfect gas $h = C_p T$)

k — thermal conductivity

M_∞ — freestream Mach number

N — exponent for $\frac{u}{u_\infty} = \left(\frac{y}{\delta}\right)^{1/N}$; this expression is fitted to as much of the experimental velocity profile as possible

Pr — Prandtl number, $\dfrac{C_p \mu}{k}$

q — energy transfer in the y-direction, per unit time per unit area (as defined by Eq. (2))

Q — total-energy deficiency of the boundary layer relative to the free stream

R — perfect gas constant

T — static temperature

T_t — total temperature

u	velocity component parallel to the plate
x	longitudinal distance along the plate
y	distance perpendicular to the plate
γ	ratio of specific heats, taken as 1.4 for air
δ	boundary-layer thickness
ϵ	eddy diffusivity of momentum
ϵ_h	eddy diffusivity of heat
θ	momentum thickness, $\int_0^\delta \frac{\rho u}{\rho_\infty u_\infty} \left(1 - \frac{u}{u_\infty}\right) dy$
μ	viscosity
ρ	density
τ	shear stress, force per unit area

Subscripts:

aw	pertaining to adiabatic wall conditions
t	total
w	pertaining to wall
∞	local free stream

I. INTRODUCTION

The ability to predict the variation of boundary-layer parameters, such as momentum, displacement, and energy thicknesses in supersonic flow, is very important in supersonic inlet design. In order to describe the distribution of these parameters, a knowledge of the turbulent boundary-layer temperature profile is needed, in addition to the velocity profile and friction coefficients.

The difficulties encountered in the theoretical evaluation, even for the zero-pressure gradient turbulent boundary layer, has resulted in the use of empirical correlations in turbulent boundary-layer analyses. For example, correlations for the compressible friction coefficient have lead to the establishing of various methods for its determination; an outline of several of these is presented in Reference 1 by Nestler and Goetz. A second example is related to the correlation of zero-pressure gradient velocity profiles; empirical correlations for incompressible flow are presented in Reference 2.

To the present time the turbulent boundary-layer temperature profile, with heat transfer, has not been successfully correlated even for the zero-pressure gradient boundary layer. The determination of turbulent boundary-layer temperature profiles has been limited, generally, to attempts at altering an expression obtained by Luigi Crocco (this expression is presented in Reference 3, by Van Driest)

for laminar flow; this method differs from that presented in Reference 4 by R. G. Deissler and A. L. Loeffler, Jr. In Reference 4 an expression for the turbulent boundary layer temperature profile is presented which is based on the differential equations for local heat transfer and shear. Before the turbulent temperature profile expression in Reference 4 can be utilized, a knowledge of the ratio of the eddy diffusivities of heat (ϵ_h) to momentum (ϵ) is necessary. It is pointed out in Reference 4 that for flow over a flat-plate the ratio of diffusivities (ϵ_h/ϵ) is very close to unity; and, therefore, most of the calculated results presented in Ref. 4 have been derived using this assumption.

A comparison of the results obtained by using the theoretical expression for the turbulent boundary-layer temperature profile (from Reference 4) with experimental data reveals that the ratio of diffusivities, $\frac{\epsilon_h}{\epsilon}$, differs appreciably from unity for some examples of flat-plate flow. An erroneous use of unity, for the ratio of diffusivities, results in incorrect total energy deficiencies for the boundary layers in question. This also leads to incorrect velocity-temperature profiles.

The present investigation is similar, in approach, to that carried out in Reference 4, but eliminates the need for assuming a particular value of $\frac{\epsilon_h}{\epsilon}$. The resulting turbulent boundary-layer velocity-temperature relationship, derived in this thesis, also produces the correct total-energy deficiencies for the boundary layers in

question. In this thesis the resulting velocity-temperature relationship is utilized to describe turbulent boundary-layer static temperature profiles; these results are compared with experimental data.

II. ANALYSIS

Classically, the turbulent boundary layer is divided into three regions:

1. The inner region or laminar sublayer;

2. The transition region between the laminar sublayer and the turbulent flow region; and

3. The turbulent flow region.

In deriving an expression for the turbulent boundary-layer enthalpy velocity distribution it was not necessary to distinguish between these three regions of the boundary layer. However, various features of two of these regions, namely the laminar sublayer and the turbulent flow region, are in evidence through the boundary conditions and the form of the equations for shear stress and heat transfer that are assumed.

From Reference 4 the local shear and energy transfer in the boundary layer can be expressed as follows:

$$\tau = (\mu + \rho\epsilon) \frac{du}{dy} \tag{1}$$

and

$$q = - \left(\frac{k}{c_p} + \rho\epsilon_h \right) \frac{dh}{dy} - (\mu + \rho\epsilon)\, u \frac{du}{dy} . \tag{2}$$

Dividing Eq. (2) by Eq. (1) and nondimensionalizing h and u with respect to the free stream gives,

$$\frac{q}{\tau} = - \frac{h_\infty}{u_\infty} \left(\frac{\frac{k}{C_p} + \rho \epsilon_h}{\mu + \rho\epsilon} \right) \frac{d\left(\frac{h}{h_\infty} \right)}{d\left(\frac{u}{u_\infty} \right)} - u_\infty \left(\frac{u}{u_\infty} \right) , \qquad (3)$$

In order to integrate Eq.(3) a knowledge of the relationships between $\frac{q}{\tau}$ and u and between $\left(\frac{\frac{k}{C_p} + \rho \epsilon_h}{\mu + \rho\epsilon} \right)$ and h is needed. Here the ratio $\left(\frac{\frac{k}{C_p} + \rho \epsilon_h}{\mu + \rho \epsilon} \right)$ is assumed to be constant and is designated "a."

From a consideration of the boundary conditions imposed on the governing equations (which are presented in Appendix A of Reference 4) when a constant wall temperature is assumed,

$$\left(\frac{\partial \tau}{\partial y} \right)_w = \left(\frac{\partial q}{\partial y} \right)_w = 0 \qquad (4)$$

and

$$\left(\frac{\partial^2 \tau}{\partial y^2} \right)_w = \left(\frac{\partial^2 q}{\partial y^2} \right)_w = 0 \quad , \qquad (5)$$

a polynomial of the form,

$$\frac{q}{\tau} = b + c \left(\frac{u}{u_\infty} \right)^3 \qquad (6)$$

is assumed for the q/τ relationship with the velocity profile.

Substituting $\frac{\frac{k}{C_p} + \rho \epsilon_h}{\mu + \rho\epsilon} = a$, and Eq. (6), into Eq.(3) and integrating from the wall to an arbitrary point in the boundary layer gives, after rearranging,

$$\frac{h}{h_\infty} = \frac{h_w}{h_\infty} - \frac{u_\infty^2}{h_\infty} \left[\frac{b}{a u_\infty} \left(\frac{u}{u_\infty} \right) + \frac{1}{2a} \left(\frac{u}{u_\infty} \right)^2 + \frac{c}{4a u_\infty} \left(\frac{u}{u_\infty} \right)^4 \right] . \quad (7)$$

The constants a, b, and c in Eq. (7) are determined from the boundary conditions (constants a, b and c are really functions of x),

1. From Reynolds analogy,

$$\left[\frac{d \frac{h}{h_\infty}}{d \frac{u}{u_\infty}} \right]_w = \left(\frac{h_{aw} - h_w}{h_\infty} \right) Pr^{1/3} .$$

2. At the outer edge of the boundary-layer it is assumed $\frac{h}{h_\infty} = 1.0$ and $\frac{u}{u_\infty} = 1.0$.

3. The total-energy deficiency, using the expression of Appendix A and assuming $\frac{u}{u_\infty} = \left(\frac{y}{\delta} \right)^{1/N}$, is matched with the total-energy deficiency of the experimental case. (Values for the total-energy deficiency of the available experimental data are presented in Table I corresponding to Eq. (A5).) The application of boundary condition (1) to Eq. (7), is found to yield

$$\left[\frac{d\,\frac{h}{h_\infty}}{d\,\frac{u}{u_\infty}}\right]_w = -\frac{u_\infty}{h_\infty}\frac{b}{a} \quad . \tag{8}$$

The application of boundary condition (2) to Eq. (7), and substitution of Eq. (8) into the result, gives

$$\frac{u_\infty^2}{2ah_\infty} = -1 + \left[\frac{d(\frac{h}{h_\infty})}{d\,\frac{u}{u_\infty}}\right]_w + \frac{h_w}{h_\infty} + \frac{u_\infty}{4h_\infty}\left(\frac{c}{a}\right) . \tag{9}$$

The substitution of Eqs. (8) and (9) into Eq. (7) leads to

$$\frac{h}{h_\infty} = \frac{h_w}{h_\infty} + \left[\frac{d(\frac{h}{h_\infty})}{d(\frac{u}{u_\infty})}\right]_w \left(\frac{u}{u_\infty}\right) + \left\{1 - \left[\frac{d(\frac{h}{h_\infty})}{d(\frac{u}{u_\infty})}\right]_w - \frac{h_w}{h_\infty} + \frac{u_\infty}{4h_\infty}\frac{c}{a}\right\}\left(\frac{u}{u_\infty}\right)^2$$

$$- \frac{u_\infty}{4h_\infty}\left(\frac{c}{a}\right)\left(\frac{u}{u_\infty}\right)^4 , \tag{10}$$

and the rearrangement of Eq. (10) gives,

$$\frac{h}{h_\infty} = \frac{h_w}{h_\infty} + \left(1 - \frac{h_w}{h_\infty}\right)\left(\frac{u}{u_\infty}\right)^2 + \left[\frac{u}{u_\infty} - \left(\frac{u}{u_\infty}\right)^2\right]\left[\frac{d(\frac{h}{h_\infty})}{d(\frac{u}{u_\infty})}\right]_w$$

$$+ \frac{u_\infty}{4h_\infty}\left(\frac{c}{a}\right)\left[\left(\frac{u}{u_\infty}\right)^2 - \left(\frac{u}{u_\infty}\right)^4\right] . \tag{11}$$

Applying boundary condition (3) and matching the boundary-layer total-energy deficiencies (obtained from experimental and theoretical studies) suggests a correct value for the parameter $\frac{u_\infty}{4h_\infty}\left(\frac{c}{a}\right)$ in Eq. (11). Equation (11) then gives the enthalpy-velocity relation which, after being combined with the power law velocity profile used here, produces the correct total-energy deficiency of the boundary layer in question.

Assuming a perfect gas (for which $h = C_pT$) Eq. (11) can be rearranged to give,

$$\frac{T}{T_\infty} = \frac{T_w}{T_\infty} + \left(1 - \frac{T_w}{T_\infty}\right)\left(\frac{u}{u_\infty}\right)^2 + \left[\frac{u}{u_\infty} - \left(\frac{u}{u_\infty}\right)^2\right]\left[\frac{d\left(\frac{T}{T_\infty}\right)}{d\left(\frac{u}{u_\infty}\right)}\right]_w$$

$$+ \frac{(\gamma-1)\,M_\infty^2}{4u_\infty}\left(\frac{c}{a}\right)\left[\left(\frac{u}{u_\infty}\right)^2 - \left(\frac{u}{u_\infty}\right)^4\right]. \qquad (12)$$

III. RESULTS AND DISCUSSION

In the present analysis a power law velocity profile has been assumed. In order to determine the effect of assuming various power law velocity profiles, temperature versus velocity profiles were determined corresponding to one experimental example assuming power law profiles of $\frac{u}{u_\infty} = \left(\frac{y}{\delta}\right)^{1/6}$ and $\frac{u}{u_\infty} = \left(\frac{y}{\delta}\right)^{1/8}$. The results of these calculations are presented in Figure 1 with the corresponding experimental temperature $\left(\frac{T}{T_\infty}\right)$ versus velocity $\left(\frac{u}{u_\infty}\right)$ profile (from Reference 5).

Figure 1 shows that theoretical temperature versus velocity profile is a weak function of the power law velocity profile assumed. As the resulting effect of the assumed power law velocity profile is deemed to be of a minor nature, the remainder of the theoretical $\left(\frac{T}{T_\infty} \text{ versus } \frac{u}{u_\infty}\right)$ curves, of Figures 2 through 6 (from Reference 5 and 6) are calculated using the velocity profile, $\frac{u}{u_\infty} = \left(\frac{y}{\delta}\right)^{1/7}$. Figures 1 through 6 show that the theoretical temperature-velocity profiles do correspond well with experimental data.

As Figure 1 indicates, the theoretical curves of $\frac{T}{T_\infty}$ versus $\frac{u}{u_\infty}$ are weak functions of the velocity profile assumed, it is necessary to consider the effect of ignoring the use of the velocity profile of the laminar sublayer in the theoretical calculations. In the comparison

of the present experimental curves ($\frac{T}{T_\infty}$ versus $\frac{u}{u_\infty}$) with the theoretical results, ignoring the laminar sublayer velocity profile did not seem to significantly affect the correlation between the theoretical results and the experimental data. The absence of any effect resulting from not considering the laminar sublayer velocity profile when computing the theoretical curves of $\frac{T}{T_\infty}$ versus $\frac{u}{u_\infty}$ is believed to be due to the existence of thin laminar sublayers. The laminar sublayers of the available experimental data make up, approximately, only five to ten percent of the boundary-layer velocity profiles based on boundary layer thickness. Thus, it is believed that the use of an assumed power law velocity profile, in the theoretical calculations, must be restricted to turbulent boundary layers with relatively thin laminar sublayers.

As pointed out in the introduction most previous attempts to express the relationship between the turbulent boundary-layer temperature and velocity profiles have been limited to attempts at altering the expression obtained by Crocco for laminar flow. A typical example of these temperature-velocity profile relationships (Reference 7) is,

$$\frac{T}{T_\infty} = 1 + \frac{\gamma-1}{2} Pr^{1/3} M_\infty^2 \left[1 - \left(\frac{u}{u_\infty}\right)^2\right] + \frac{T_w - T_{aw}}{T_\infty}\left[1 - \left(\frac{u}{u_\infty}\right)\right] . \quad (13)$$

A comparison of experimental data with the results obtained using Eq. (13), for the temperature-velocity relationship, revealed that a

satisfactory correlation with experimental profiles was obtained when two specific conditions existed in the experimental data. First, that the energy deficiency is practically zero, and second, that the wall temperature is close, in value, to the adiabatic wall temperature.

A comparison of the adiabatic expressions of Eqs. (11) and (13) revealed the difference to be the term $\frac{u_\infty}{4h_\infty}\left(\frac{c}{a}\right)\left[\left(\frac{u}{u_\infty}\right)^2-\left(\frac{u}{u_\infty}\right)^4\right]$, and this term was found to be negligible for zero energy deficiencies with the corresponding adiabatic walls. Thus, the correspondence of the results obtained using Eq. (13) with essentially adiabatic turbulent boundary layers is a result of the fact that the last term of Eq. (11) is negligible under these governing conditions.

The derivation of Eq. (13) has as its basis the assumption of the existence of a constant flat-plate surface temperature and free-stream Mach number from the plate leading edge to the station in question. Based on these assumptions, Reynolds analogy gives (for a perfect gas) the total-energy deficiency at the station in question as

$$Q = \frac{\rho_\infty u_\infty c_{p\infty} T_\infty}{Pr^{2/3}}\left(\frac{T_{aw}-T_w}{T_\infty}\right)\theta\ , \tag{14}$$

or solving for $\frac{T_w}{T_\infty}$, as

$$\frac{T_w}{T_\infty} = \frac{T_{aw}}{T_\infty} - \frac{Pr^{2/3}\,Q}{T_\infty \rho_\infty u_\infty c_{p_\infty}\theta}\ . \tag{15}$$

Based on the above observations for flat-plate flow it is believed that good correspondence between experimental data and the theoretical results, using Eq. (13), can be obtained when $\frac{T_w}{T_\infty}$, Q, and θ correspond in the manner presented in Eq. (15); this corresponds to ideal flat-plate flow. As a measure of the deviation from ideal flat-plate flow of the experimental data of Figures 1 through 6, the value of $\frac{T^*_w}{T_\infty}$ is calculated using Eq. (15) in conjunction with the value of $\frac{Q\ Pr^{2/3}}{T_\infty \rho_\infty u_\infty c_{p_\infty} \theta}$ given in Table I for each experimental temperature-velocity profile. The effective wall temperature, T^*_w, thus obtained is the value of wall temperature, T_w, which would be required to produce the total-energy deficiency on a flat plate at the local free-stream conditions and local boundary-layer momentum thickness (that is, for ideal flat-plate flow). The resulting difference between $\frac{T^*_w}{T_\infty}$ and $\frac{T_w}{T_\infty}$ of each example experimental data point is a measure of the deviation from ideal flat-plate flow of the experimental data in Figures 1 through 6.

The values of $\frac{T^*_w}{T_\infty}$ for the experimental data in Figures 1 through 6 are presented in Table I. These values of $\frac{T^*_w}{T_\infty}$ are combined with $\frac{T_w}{T_\infty}$ to determine the value of $\frac{\frac{T_w}{T_\infty} - \frac{T^*_w}{T_\infty}}{\frac{T^*_w}{T_\infty}}$ for each experimental temperature-velocity profile and the results are plotted in Figure 7 versus

$$\frac{\left(\frac{T}{T_\infty}\right)_{\text{data}} - \left(\frac{T}{T_\infty}\right)_{\text{Ref. 7}}}{\left(\frac{T}{T_\infty}\right)_{\text{Ref. 7}}}$$

. The value of $\left(\frac{T}{T_\infty}\right)_{\text{data}}$ and $\left(\frac{T}{T_\infty}\right)_{\text{Ref. 7}}$ used in Figure 7 was chosen at the point in the boundary layer where,

$$\frac{u}{u_\infty} \cong 12\sqrt{\frac{T_w}{T_\infty}\frac{C_f}{2}} \quad . \tag{16}$$

Equation (16) identifies the edge of the laminar sublayer as given by turbulent boundary layer theory (Reference 2). The value of C_f used in Eq. (16) was determined for each experimental data point using Eckert's reference temperature method as presented in Reference 1. The value of $\frac{u}{u_\infty}$ corresponding to Eq. (16) is identified on each experimental temperature-velocity profile figure (Figs. 1 through 6). Figure 7 shows that the best correspondence with the experimental temperature-velocity profiles of Figures 1 through 6 should be the profiles of Figures 1 and 3 since these profiles have values of $\frac{\frac{T_w}{T_\infty} - \frac{T^*_w}{T_\infty}}{\frac{T^*_w}{T_\infty}}$ closest to zero.

Temperature-velocity profiles corresponding to Eq. (13) are presented on Figures 1 through 6 corresponding to each experimental temperature-velocity profile. As was indicated in Figure 7,

Figures 1 and 3 show the best correspondence of temperature-velocity profiles, generated using Eq. (13), with the experimental temperature-velocity profiles.

IV. CONCLUDING REMARKS

The present method for computing the static-temperature versus velocity distribution for a zero pressure gradient turbulent boundary layer with heat transfer gives results which correlate well with available experimental data. In the analytical method, a power law turbulent boundary layer velocity profile was assumed. It was observed that the analytical results are a weak function of the power law velocity profile assumed. The experimental velocity profiles, for which the power law assumption gives good correspondence, are restricted to turbulent boundary layers which have thin laminar sublayers. Therefore this assumption of the power law velocity profile restricts the method so that it can be applied, most satisfactorily, to turbulent boundary layers with relatively thin laminar sublayers. A comparison of experimental temperature-velocity profiles with standard flat-plate turbulent boundary-layer temperature-velocity relations revealed that correlation with experimental profiles is obtained when the experimental data correspond to ideal flat-plate flow. Here an ideal flat-plate flow has constant free-stream properties and plate temperature over the length of plate upstream of the station where the experimental temperature-velocity profile in question was measured.

V. SUMMARY

An expression for the relationship between the static temperature and the velocity in a turbulent boundary layer is derived based on differential equations for the local heat transfer and shear. The boundary conditions imposed by these governing equations showed the static temperature-velocity relation to be at least a fourth degree polynomial which differs considerably from the second degree polynomial obtained by previous investigators. These governing equations are integrated using as boundary conditions the total energy deficiency of the boundary layer, the slope at the wall of the laminar sublayer temperature velocity relation (as determined using Reynolds analogy), and the local freestream conditions. Results obtained by this method are compared with available experimental temperature-velocity profile data and found to correlate well with the experimental profiles.

VI. ACKNOWLEDGMENTS

The author wishes to extend his appreciation to John R. Henry, of the National Aeronautics and Space Administration, Langley Research Center, for his advice during the development of the analytical method for predicting the static temperature distribution in a turbulent boundary layer with heat transfer.

The author also is indebted to Dr. F. R. DeJarnette and Dr. J. B. Eades, Jr., both of Virginia Polytechnic Institute, for their suggestions of the best method of presenting the present material, as well as their advice for improving the technical correctness of this thesis.

The author wishes to thank his wife, Evelyn A. Pinckney, for her help with the preparation of the figures and the proofreading of the manuscript. Thanks for the typing of the manuscript is extended to Mrs. Jane Johnston of Virginia Polytechnic Institute.

VII. REFERENCES

1. Nestler, D. E.; and Goetz, R.: Survey of Theoretical and Experimental Determinations of Skin Friction in Compressible Boundary Layers. Part II - The Turbulent Boundary Layer on a Flat Plate. General Electric Co., Thermodynamics Tech. Memo. No. 109, January 29, 1959.

2. Cornish, Joseph Jenkins, III: A Universal Description of Turbulent Boundary-Layer Profiles with or without Transpiration. The Aero-Physics Dept. of Mississippi State Univ., Res. Rept. No. 29, June 1, 1960.

3. Van Driest, E. R.: Investigation of Laminar Boundary Layer in Compressible Fluids Using the Crocco Method. NACA TN 2597, January 1952.

4. Deissler, R. G.; and Loeffler, A. L., Jr.: Analysis of Turbulent Flow and Heat Transfer on a Flat Plate at High Mach Numbers with Variable Fluid Properties. NASA TR R-17, 1959.

5. Kepler, C. E.; and O'Brien, R. L.: Supersonic Turbulent Boundary Layer Growth over Cooled Walls in Adverse Pressure Gradients. Tech. Doc. Rept. No. ASD TDR 62-87, United Aircraft Corp., October 1962.

6. Lobb, R. Kenneth; Winkler, Eva M.; and Persh, Jerome: Experimental Investigation of Turbulent Boundary Layers in Hypersonic Flow. Presented at 22nd Annual Meeting, January 25-29, 1954, Inst. of the Aero. Sci., Preprint No. 452.

7. Persh, Jerome; and Lee, Roland: Tabulation of Compressible Turbulent Boundary Layer Parameters. Aeroballistics Res. Rept. 337, NAVORD Rept. 4282, May 1956.

VIII. VITA

The author was born on September 21, 1934 in Chipley, Florida. He graduated from St. Petersburg High School in June 1952 and obtained a Bachelor of Science Degree in mathematics from Florida State University in June 1957. After graduation from Florida State University he was employed as a research engineer by the National Advisory Committee for Aeronautics, now the National Aeronautics and Space Administration, at their Langley Research Center. In June 1964 he obtained a Master of Science Degree in mathematics from Virginia Polytechnic Institute. At the writing of this thesis he is still employed by the National Aeronautics and Space Administration as a research engineer at the Langley Research Center.

Shirley J. Pinckney

IX. APPENDIX A

EQUATION FOR TOTAL-ENERGY DEFICIENCY

The total-energy transferred to the wall upstream of a particular boundary-layer station can be obtained by the integration of the energy deficiency of the boundary layer relative to the free stream. The result is

$$Q = \int_0^{\delta} \rho\, u h_{t,\infty}\, dy - \int_0^{\delta} \rho\, u h_t\, dy \qquad \text{(A1)}$$

After rearranging, Eq. (A1) becomes

$$Q = \rho_\infty u_\infty \delta \left[h_{t,\infty} \int_0^1 \frac{\rho u}{\rho_\infty u_\infty} d\left(\frac{y}{\delta}\right) + \int_0^1 \frac{\rho u}{\rho_\infty u_\infty} h_t d\left(\frac{y}{\delta}\right) \right]. \qquad \text{(A2)}$$

The second term in the parentheses on the right-hand side of Eq. (A2) can also be expressed as

$$\int_0^1 \frac{\rho u}{\rho_\infty u_\infty} h_t d\left(\frac{y}{\delta}\right) = \int_0^1 \frac{\rho u}{\rho_\infty u_\infty} \left[h + \frac{u^2}{2} \right] d\left(\frac{y}{\delta}\right)$$

$$= h_\infty \int_0^1 \frac{\rho u}{\rho_\infty u_\infty} \left(\frac{h}{h_\infty}\right) d\left(\frac{y}{\delta}\right) + \frac{1}{2} u_\infty^2 \int_0^1 \frac{\rho u^3}{\rho_\infty u_\infty^2} d\left(\frac{y}{\delta}\right). \qquad \text{(A3)}$$

Substituting Eq. (A3) into Eq. (A2) one obtains

$$Q = \rho_\infty u_\infty \delta \left[h_{t,\infty} \int_0^1 \frac{\rho u}{\rho_\infty u_\infty} d\left(\frac{y}{\delta}\right) + \right.$$

$$\left. h_\infty \int_0^1 \frac{\rho u h}{\rho_\infty u_\infty h_\infty} d\left(\frac{y}{\delta}\right) + \frac{u_\infty^2}{2} \int_0^1 \frac{\rho u^3}{\rho_\infty u_\infty^3} d\left(\frac{y}{\delta}\right) \right] . \qquad \text{(A4)}$$

For a perfect gas $h = c_p T$, and c_p is constant. Assuming a perfect gas, Eq. (A4) can be rearranged to yield

$$\frac{Q}{\rho_\infty u_\infty c_{p,\infty} T_{t,\infty} \delta} = \int_0^1 \frac{\rho u}{\rho_\infty u_\infty} d\left(\frac{y}{\delta}\right) - \left(\frac{T}{T_t}\right)_\infty \left[\int_0^1 \frac{u}{u_\infty} d\left(\frac{y}{\delta}\right) + \right.$$

$$\left. \frac{\gamma - 1}{2} M_\infty^2 \int_0^1 \frac{\rho u^3}{\rho_\infty u_\infty^3} d\left(\frac{y}{\delta}\right) \right] . \qquad \text{(A5)}$$

Figure	Pr	M_∞	Ref.	$\frac{T_w}{T_\infty}$	$\frac{T_{aw}}{T_\infty}$	$\frac{Q}{\rho_\infty u_\infty c_{p,\infty} T_{t,\infty} \delta}$	$\frac{Q\ Pr^{2/3}}{\rho_\infty u_\infty c_{p,\infty} T_\infty \theta}$	$\frac{T_w^*}{T_\infty}$
1	0.725	3.00	5	1.316	2.612	0.0293	0.857	1.755
2	0.725	6.78	6	4.640	9.270	0.0412	8.044	1.226
3	0.725	5.01	6	4.310	5.540	0.0216	2.377	3.163
4	0.725	5.06	6	3.270	5.630	0.0387	4.155	1.475
5	0.725	6.00	5	2.210	7.450	0.0164	2.667	4.780
6	0.725	6.83	6	6.340	9.350	0.0264	5.914	3.436

BOUNDARY CONDITIONS FOR THE EXPERIMENTAL DATA

TABLE I

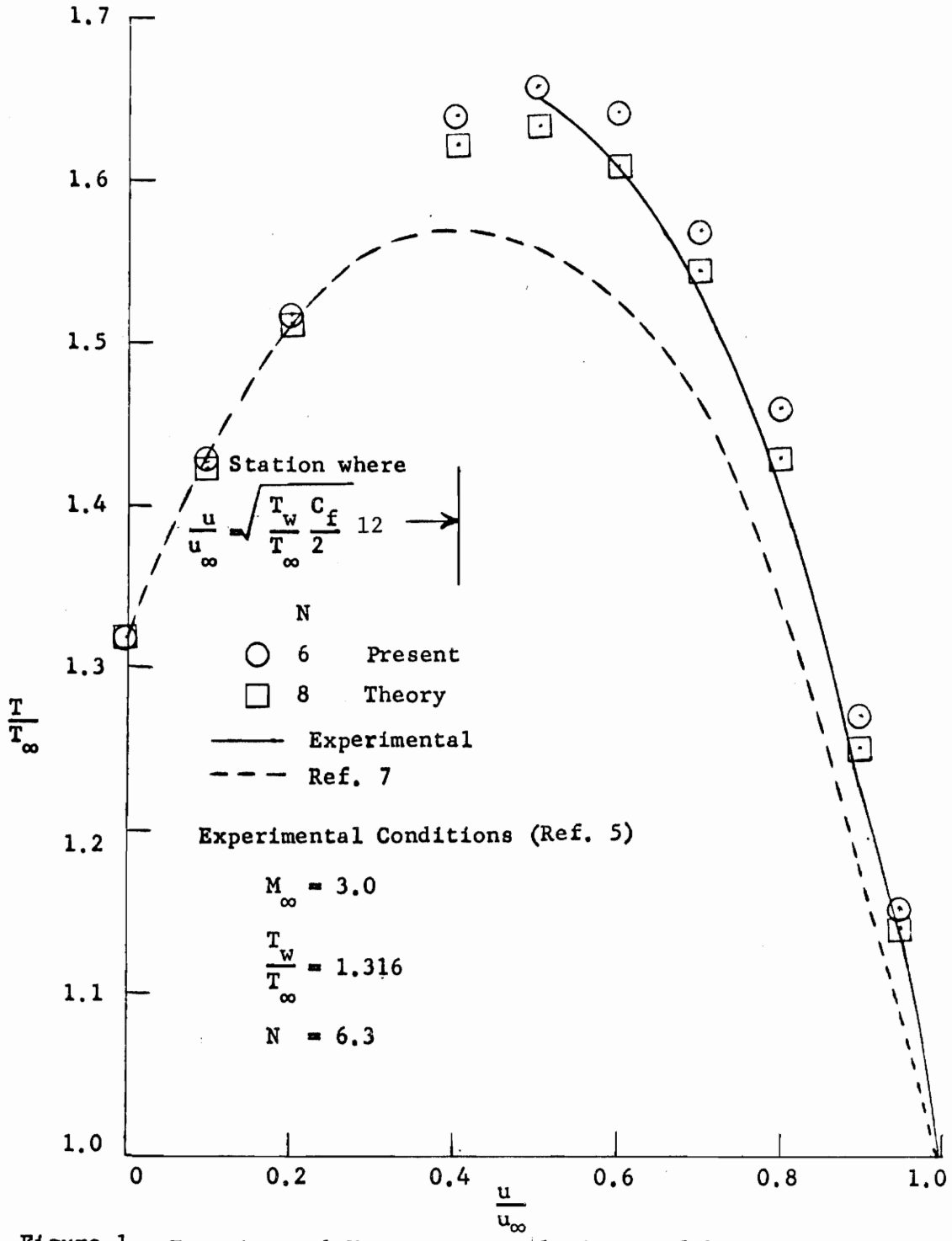

Figure 1. Experimental Temperature-Velocity Profile Compared with Results from the Present Method and with Reference 7

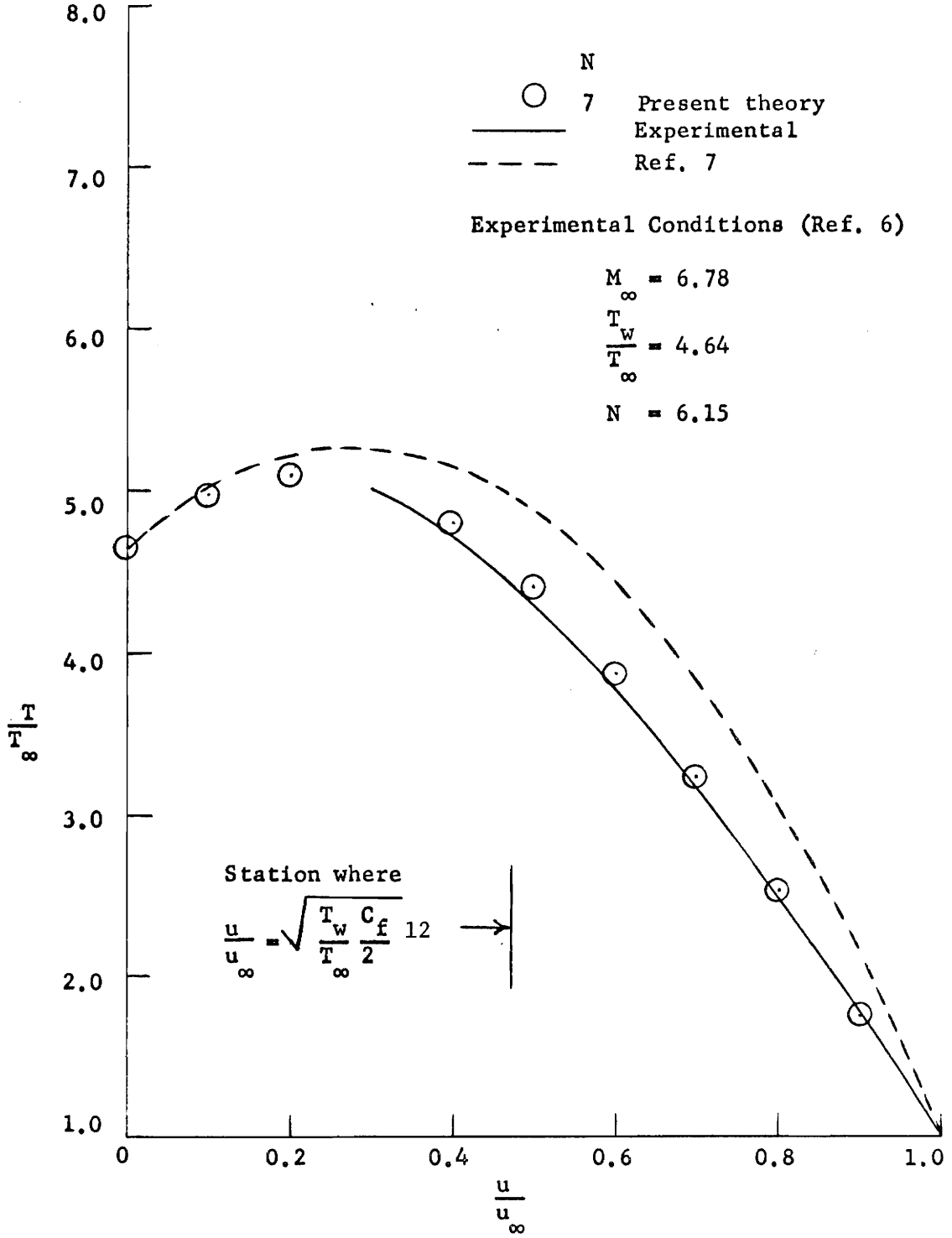

Figure 2. Experimental Temperature-Velocity Profile Compared with the Present Method and with Reference 7

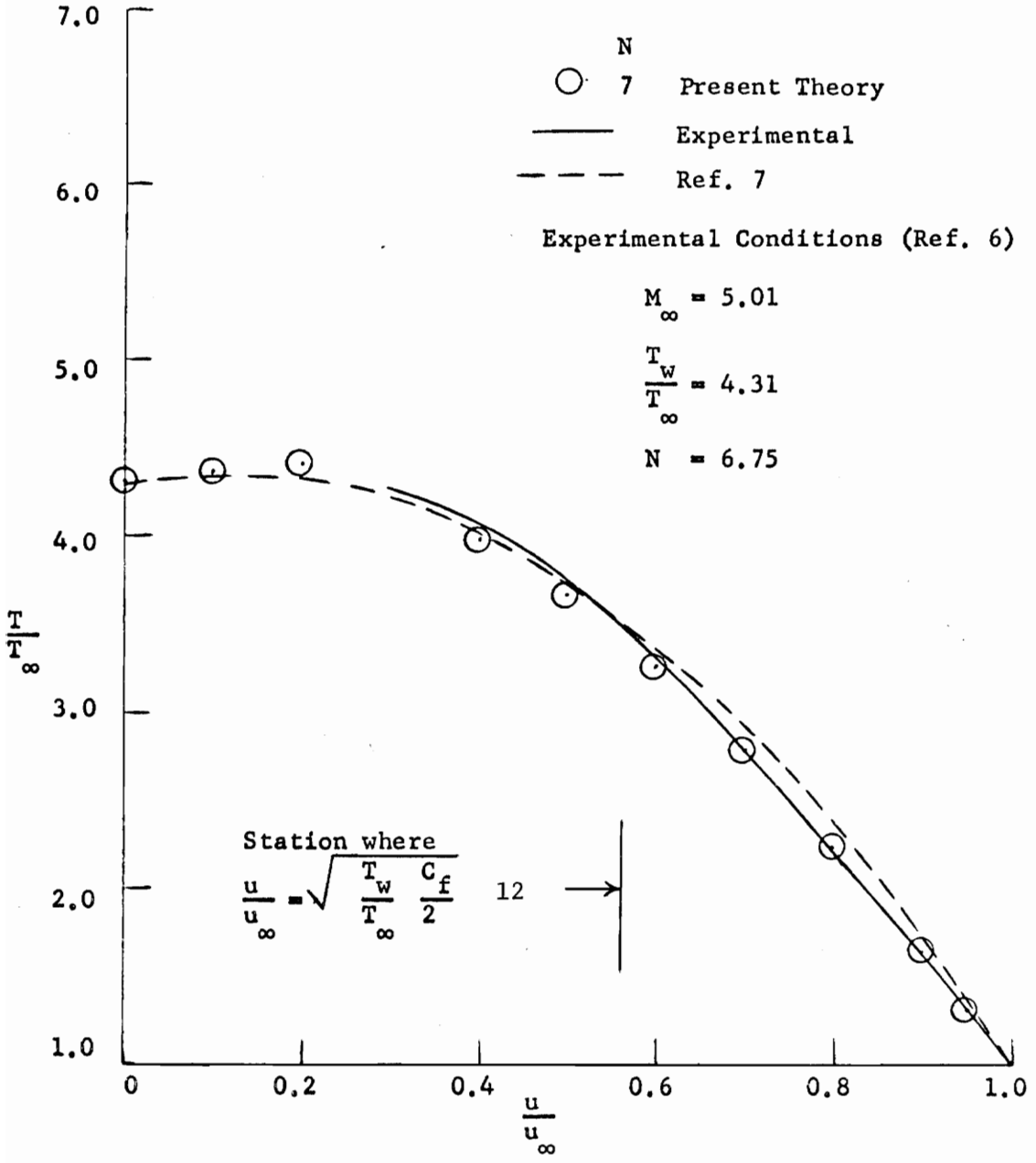

Figure 3. Experimental Temperature-Velocity Profile Compared with Results from the Present Method and with Reference 7

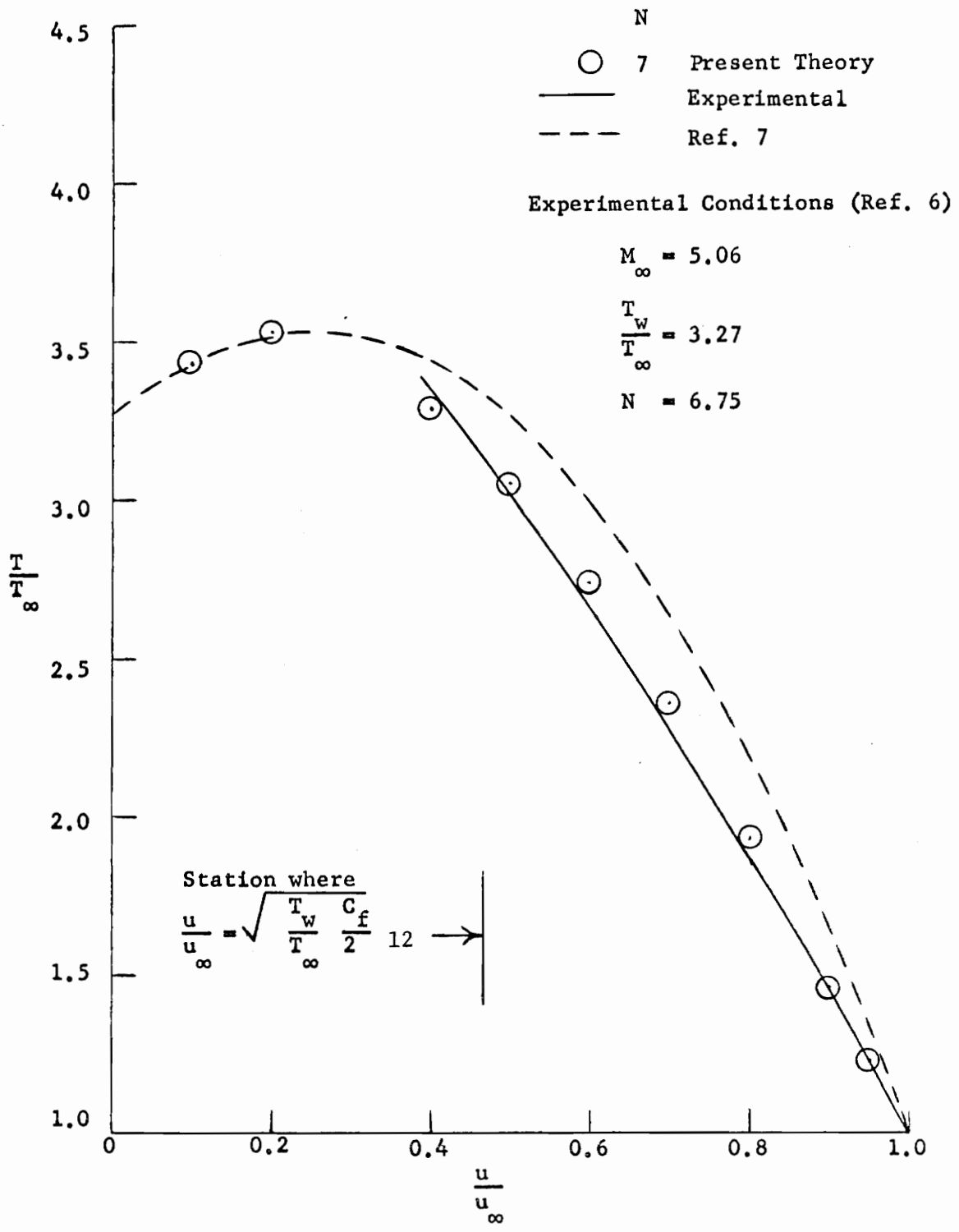

Figure 4. Experimental Temperature-Velocity Profile Compared with the Present Method and with Reference 7

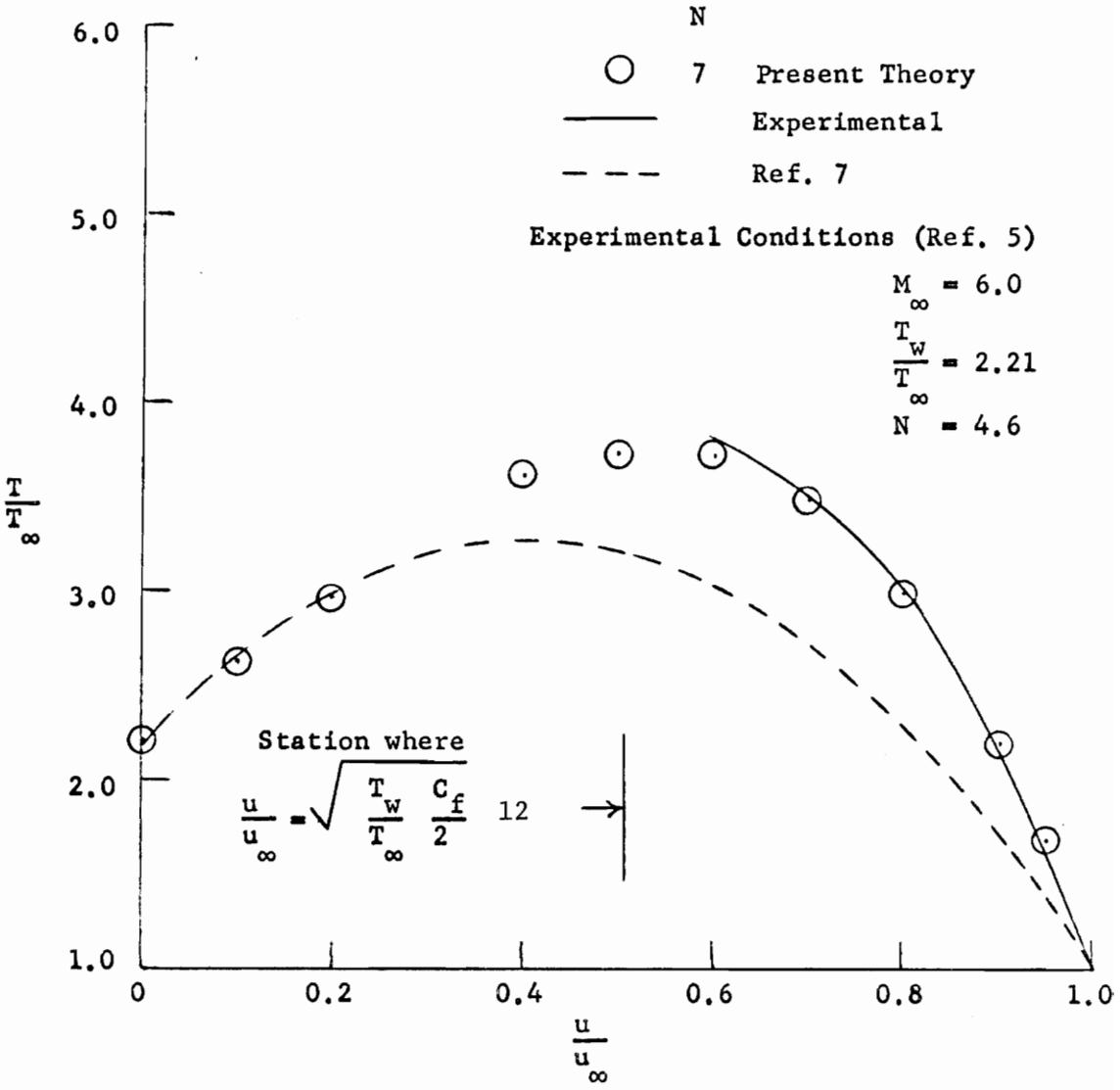

Figure 5. Experimental Temperature-Velocity Profile Compared with Results from the Present Method and with Reference 7

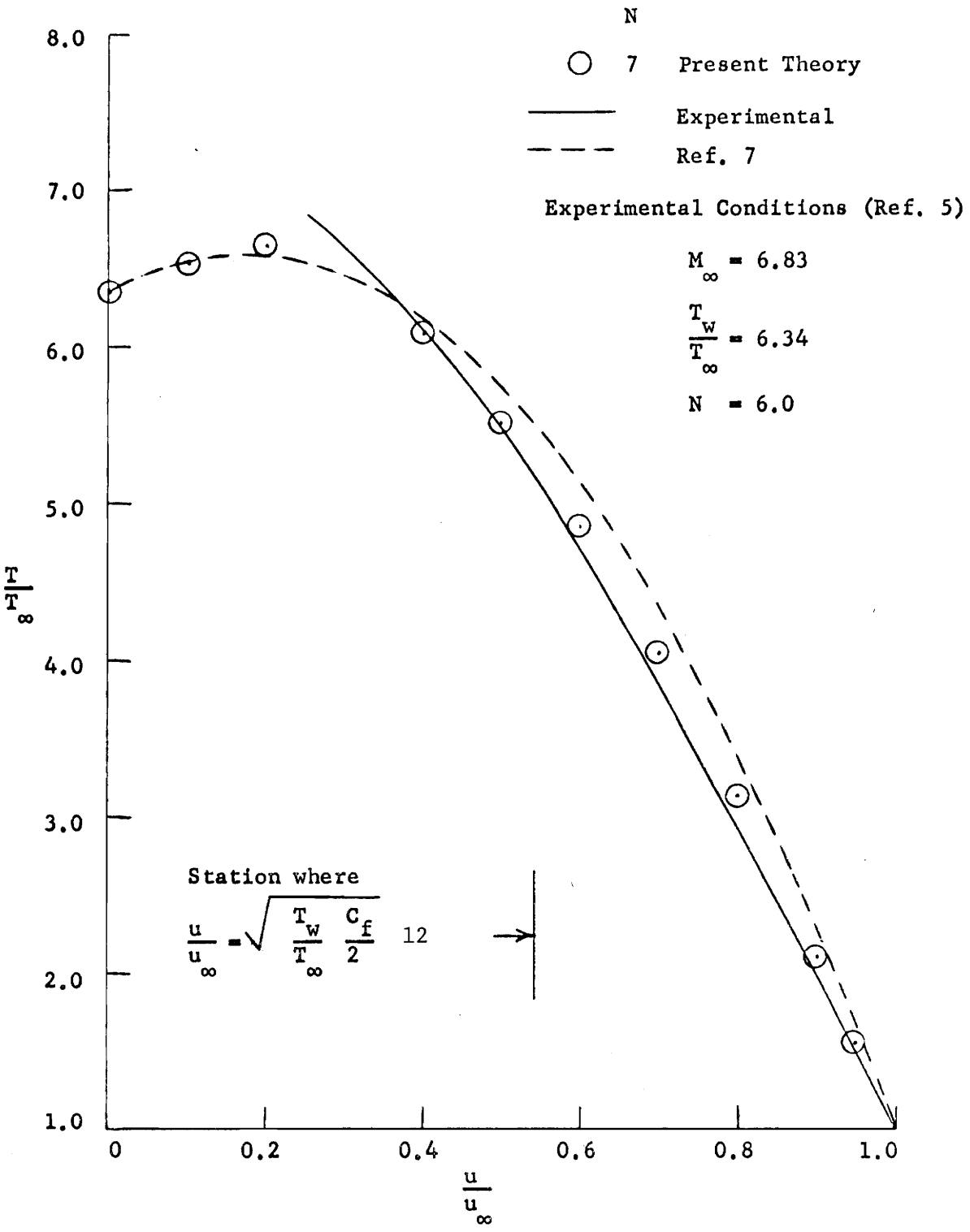

Figure 6. Experimental Temperature-Velocity Profile Compared with the Present Method and with Reference 7

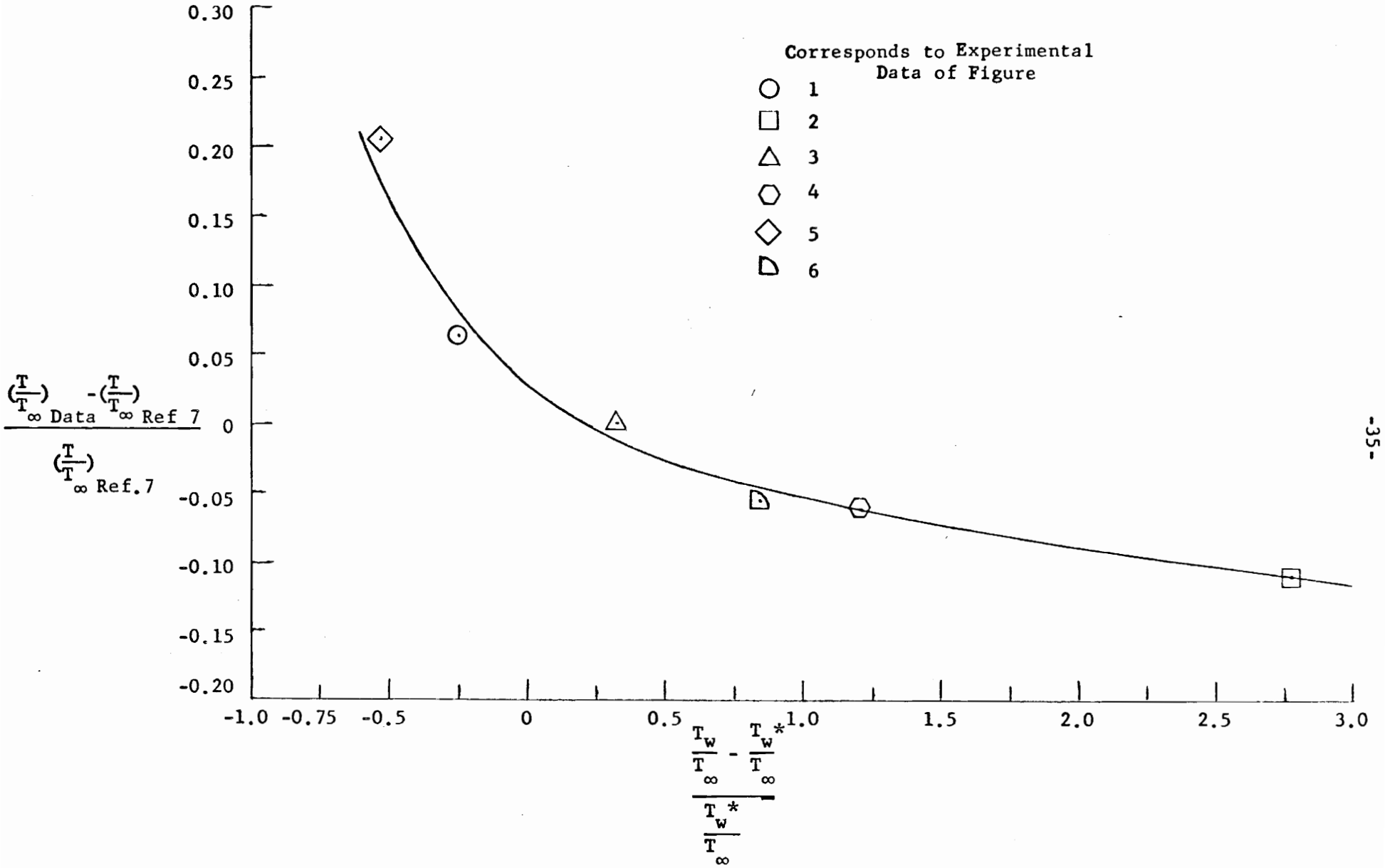

Figure 7. The Deviation of Experimental Turbulent Boundary Layer Data (Figs. 1 through 6) from an Ideal Flat Plate Flow

FLAT PLATE TURBULENT BOUNDARY LAYER STATIC TEMPERATURE DISTRIBUTION WITH HEAT TRANSFER

by

Shimer Z. Pinckney

ABSTRACT

An expression for the static temperature-velocity distribution for a zero pressure gradient turbulent boundary layer is derived based on the differential equations for local heat transfer and shear. The present theoretical method of computation is found to give results which correspond well with available experimental temperature velocity distributions.